JACS
JOURNAL OF THE AMERICAN CHEMICAL SOCIETY
Article
pubs.acs.org/JACS

Regulation of DNA Strand Displacement Using an Allosteric DNA Toehold

Xiaolong Yang, Yanan Tang, Sarah M. Traynor, and Feng Li*

Department of Chemistry, Centre for Biotechnology, Brock University, St. Catharines, Ontario Canada, L2S 3A1

Supporting Information

ABSTRACT: Toehold-mediated DNA strand displacement is the fundamental basis for the construction and operation of diverse DNA devices, including circuits, machines, sensors, and reconfigurable structures. Controllable activation and regulation of toeholds are critical to construct devices with multistep, autonomous, and complex behaviors. A handful of unique toehold activation mechanisms, including toehold-exchange, associative toehold, and remote toehold, have been developed and are often combined to achieve desired strand displacement behaviors and functions. Here we report an allosteric DNA toehold (A-toehold) design that allows the flexible regulation of DNA strand displacement by splitting an input strand into an A-toehold and branch migration domain. Because of its simplicity, the A-toehold mechanism can be a useful addition to the current toolbox of DNA strand displacement techniques. We demonstrated that A-toehold enabled a number of interesting functions that were previously shown using more sophisticated DNA strand displacement systems, including (1) continuously tuning the rate of strand displacement, (2) dynamic control of strand displacement reactions, and (3) selective activation of multiple strand displacement reactions. Moreover, by combining A-toehold and toehold-exchange mechanisms, we have successfully constructed a noncovalent DNA catalysis network that resembles an allosteric enzyme.

INTRODUCTION

The remarkable programmability and specificity offered by the Watson−Crick base pairing principle make DNA a leading material for constructing nanoscale devices of varying complexity and functionality.[1] The dynamic operations of most DNA devices, including circuits,[2] machines,[3] sensors,[4] and reconfigurable structures,[5] rely on networks of DNA strand-exchange reactions in which an invading strand displaces a target strand from a DNA duplex. However, the rates of strand-exchange reactions between stable DNA duplexes and identical invading strands are very slow.[6] To overcome this kinetic barrier, Yurke et al. introduced the concept of toehold-mediated DNA strand displacement in their seminal work in 2000,[7] where a short sticky end called DNA toehold was designed into the duplex and a corresponding short complementary segment into the invading DNA (Scheme 1A). This simple yet powerful toehold design dramatically accelerates the strand-exchange rates at the branch migration (BM) domain to over 10^6 fold, leading to the origin and the boom of dynamic DNA nanotechnology.[1−7]

When using the principle of DNA toehold to guide the design and operation of a DNA device, a key mechanism is the controllable activation of a toehold.[1−7] This function is typically achieved by sequestering a toehold into an inter- or intramolecular DNA duplex, which can then be activated by external stimuli and toehold-exchange reactions.[2] To construct devices of higher complexity, cascades of toehold-exchange reactions are programmed to recognize complex environmental signals involving multiple input strands.[2] Many efforts have been made to enrich the toolbox of strand displacement techniques with alternative approaches for toehold activation.[8−10] For example, Chen described an associative DNA toehold that attached a DNA toehold to a BM domain whenever needed through hybridization, expanding the rule set to control DNA circuits.[8,9] We have previously developed a set of protein-responsive DNA toehold strategies that facilitate the design of DNA circuits for proteins.[10]

Scheme 1. Principles of Toehold-Mediated DNA Strand Displacement (A) and Allosteric Toehold-Mediated DNA Strand Displacement (B)

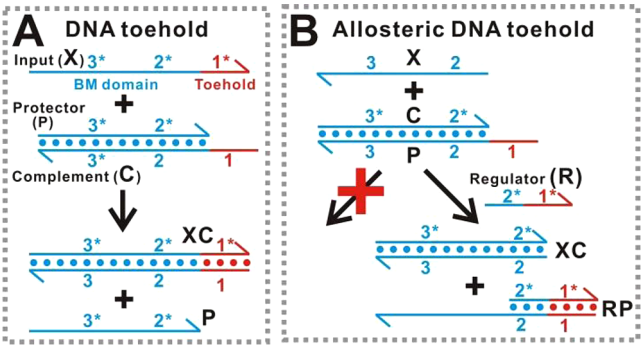

Received: August 22, 2016
Published: October 5, 2016

DOI: 10.1021/jacs.6b08794
J. Am. Chem. Soc. 2016, 138, 14076−14082

Another important consideration when using toehold to operate DNA devices is the fine adjustment of displacement rates and equilibrium concentrations.[11] Because rates of toehold-mediated strand displacements vary exponentially with the toehold length, fine adjustment on displacement kinetics is difficult.[11] Moreover, as the BM domain and the toehold are "hardwired" into the same invading strand, it is not possible to adjust kinetics without altering the equilibrium concentrations and vice versa.[8,11] Turberfield and co-workers described the concept of remote toehold that allowed additional regulation of strand displacement kinetics by introducing a linker sequence separating the toehold and BM domains.[11] However, the introduction and delicate tuning of linker domains for both invading strands and substrate strands can potentially complicate the design rules for building complex DNA network systems.

To simplify the design of complex strand displacement systems with fewer molecular components and to achieve the flexible control over the strand displacement kinetics, it is worthwhile to add new toehold regulation mechanisms to the current strand displacement toolbox. To this end, we introduce an allosteric DNA toehold (A-toehold) design that allows flexible activation/regulation of DNA strand displacement reactions and continuous control of strand displacement kinetics.

■ ALLOSTERIC TOEHOLD PRINCIPLE

The principle of A-toehold is shown in Scheme 1B. Unlike the conventional DNA toehold that has been hardwired with the BM domain, A-toehold is designed into a regulator strand R which is independent of the BM domain (Table 1). R contains

Table 1. Domain Sequences[a]

domain	sequence (5′ → 3′)	length (nt)
1	GTCTCTC	7
2	AAGCGTG	7
3	TATCCCATGTGTCA	14
5	GACAGTC	7
1*	GAGAGAC	7
2*	CACGCTT	7
3*	TGACACATGGGATA	14
3a	TATCCCAT	8
3b	GTGTCA	6
3a*	ATGGGATA	8
3b*	TGACAC	6
5*	GACTGTC	7

[a]Listed domain sequences correspond to schemes in Figure 1A, Figure 4A, Figure 5A, Figure 6A, and Figure 7A.

a toehold motif (domain 1*) and a short (e.g., 7 nt) BM motif (domain 2*), whereas the input DNA X contains only the BM domain (domain 2 and 3). To initiate a strand displacement reaction, R first reacts with CP to form a reaction intermediate CPR, which then reacts with X to form XC and RP (Figure 1B). The overall A-toehold mechanism can be expressed as the following reactions:

Reaction 1: CP + R ↔ CPR

Reaction 2: CPR + X → XC + RP

The net reaction of the A-toehold system:

X + CP + R → XC + RP

Although the free energy of the hybridization between R and CP (reaction 1) is negative, the reaction is reversible and

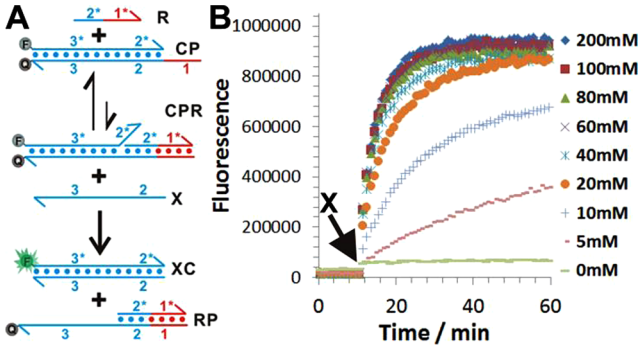

Figure 1. (A) Schematic illustration of the beacon design for real-time monitoring the A-toehold-mediated DNA strand displacement. (B) Effect of Mg^{2+} on the performance of A-toehold-mediated DNA strand displacement. [X] = 10 nM, [CP] = 20 nM, [R1] = 250 nM.

unfavorable when the concentration scale of R is low, as the number of reactants is higher than that of products. However, upon the formation of CPR triplex, the invading region of R (domain 2*) exposes a short segment of C (domain 2*) that serves as a secondary toehold to drive the strand-exchange between X and CPR (reaction 2), facilitating the net reaction.

The A-toehold design separates the toehold domain (R) from the BM domain (X) and thus allows for the independent manipulation of each domain. The A-toehold can thus be viewed as an AND gate in terms of its logic function and a join gate in terms of its role in chemical reaction networks. Compared to existing AND/join gates that are implemented with DNA strand displacements,[2] our A-toehold design is simpler and thus allows a number of interesting functions that were previously shown using more complex DNA strand displacement systems, including (1) continuous tuning the rates of strand displacement, (2) dynamic allosteric control of strand displacement reactions, (3) controllable acceleration of multiple strand displacement reactions, and (4) allosteric activation of noncovalent DNA catalysis networks.

■ MATERIALS AND METHODS

Materials and Reagents. Magnesium chloride hexahydrate ($MgCl_2·6H_2O$), sodium chloride (NaCl), 100 × Tris-EDTA (100 × TE) buffer, and TWEEN 20 solution were purchased from Sigma (Oakville, ON, Canada). Ammonium persulfate (APS), *N,N,N′,N′*-tetramethylethylenediamine (TEMED), 40% acrylamide/bis-acrylamide solution, and DNA loading buffer were purchased from Bio-Rad Laboratories, Inc. (ON, Canada). NANOpure H_2O (>18.0 MΩ), purified using an Ultrapure Milli-Q water system, was used for all experiments. All DNA samples were purchased from Integrated DNA Technologies (Coralville, IA) and purified by high-performance liquid chromatography (HPLC).

DNA Sequences and Design. DNA sequences and modifications are listed in Table S1. Sequences are based on a DNA strand displacement beacon reported by Li et al.[10a] and modified by hand to generate allosteric toehold sequences. All DNA sequences were then analyzed using NUPACK to ensure minimal crosstalk between unrelated domains.

Buffer Conditions. DNA stock solutions were prepared by dissolving oligonucleotides using 1 × TE buffer and then stored at −20 °C. Concentrations of DNA stock solutions were determined by measurement of absorbance at 260 nm using a Thermo Spectronic Unicam UV−visible spectrophotometer. Unless indicated otherwise, 1× TE buffer containing 100 mM Mg^{2+} and 0.5% v/v TWEEN 20 (referred to as TE-Mg buffer) was used as the reaction buffer. TWEEN 20 was used to prevent the potential loss of DNA oligonucleotides during dilution and pipetting.

DOI: 10.1021/jacs.6b08794
J. Am. Chem. Soc. 2016, 138, 14076−14082

Annealing. All annealing processes were performed using a BioRad T100 thermocycler. The samples (typically at a final duplex concentration of 5 μM) were heated to 95 °C for 5 min and then gradually cooled to room temperature at a constant rate over a period of 2 h.

Characterization of A-Toehold-Mediated Strand Displacement Using Spectrofluorimetry. All spectrofluorometric measurements were performed at 25 °C with a SpectraMax i3 multimode microplate reader (Molecular Devices). DNA probes C and P were labeled with a fluorophore and a quencher, respectively. CP was then annealed to make the displacement beacon at a stock concentration of 5 μM. When in use, CP was diluted using TE-Mg buffer to a final concentration of 20 nM. For a typical A-toehold-mediated strand displacement reaction, the reaction mixture contained 20 nM CP, varying concentrations of R, and varying concentrations of X in TE-Mg buffer. All reaction mixtures were prepared at a final volume of 100 μL in a 96-well microplate. Fluorescence was monitored in real-time with excitation/emission wavelength at 485 nm/515 nm at a frequency of 1 data point per minute. The measured fluorescence was normalized so that 1 normalized unit (n.u.) of fluorescence corresponded to fluorescence signal generated by 1 nM X. This normalization was achieved by using a positive control (P.C.) containing 10 nM X, 20 nM CP, and 250 nM R1 in TE-Mg buffer, and a negative control (N.C.) containing identical reagents in P.C. except that there was no X added. Fluorescence signals at t = 60 min were used for P.C. and N.C. for the normalization. When R is in large excess, the effective rate constant k_{eff} can then be estimated using the following second-order rate equation (eq 1):

$$\ln\left(\frac{[CP][X]_0}{[X][CP]_0}\right) = \ln\left(\frac{([CP]_0 - [CP]_t)[X]_0}{([X]_0 - [X]_t)[CP]_0}\right) = k_{eff}([CP]_0 - [X]_0)t \quad (1)$$

where $[CP]_0$ and $[X]_0$ are initial concentrations of reactants CP and X, $[CP]$ and $[X]$ are the concentrations of CP and X at time t, $[CP]_t$ and $[X]_t$ are the reacted concentrations of CP and X at time t.

Dynamic Regulation of Strand Displacement Using A-Toehold. The reaction mixture contained 20 nM CP displacement beacon and 10 nM input X in TE-Mg buffer and was transferred into a 96-well microplate. The fluorescence was then recorded every 1 min for 10 min. Regulator R was then quickly added into the reaction mixture at a final concentration of 20 nM. The fluorescence was then measured every 1 min for another 5 min. After 5 min, inhibitor I was then added at a final concentration of 40 nM and the fluorescence was recorded for another 10 min. The cycles for adding R and I were then repeated, and the effective concentration of R ($[R]_{eff}$) was maintained to be 20 nM and the effective concentration of I ($[I]_{eff}$) was also maintained to be 20 nM.

Selective Activation of Multiple Strand Displacement Reactions Using A-Toeholds. The reaction mixture contained 20 nM 6-FAM-labeled C1P1 displacement beacon, 20 nM TAMRA-labeled C2P2 displacement beacon, and 10 nM input X in TE-Mg buffer and was transferred into a 96-well microplate. R1 or R2 was then added to the reaction mixture at a final concentration of 100 nM. The fluorescence was then monitored using the multimode microplate reader at both "FAM channel" (485 nm/515 nm) and "TAMRA channel" (535 nm/585 nm) every 1 min for 1 h.

Allosteric Regulation of Noncovalent DNA Catalysis. The reaction mixture contained 20 nM CP, 20 nM Y, and 2 nM catalyst X_{cat} in TE-Mg buffer and was transferred into a 96-well microplate. The fluorescence was then monitored using the multimode microplate reader every 1 min for 10 min. The allosteric regulator R1 was then quickly added into the reaction mixture at a final concentration of 150 nM. The fluorescence was then monitored for another 2 h. The measured fluorescence was normalized so that 1 n.u. of fluorescence corresponded to the fluorescence signal generated by 1 nM X (r = 0). This normalization was achieved by using a P.C. containing 2 nM X, 20 nM CP, and 250 nM R1 in TE-Mg buffer, and a N.C. containing identical reagents in P.C. except that there was no X added. The turnover number (TON) was calculated using the following equation (eq 2):

$$\mathrm{TON} = \frac{[CY] + [X_{cat}C]}{[X_{cat}]} = \frac{F_{cat} - B_{cat}}{X_{cat}} \quad (2)$$

where F_{cat} is the normalized fluorescence from the reaction mixture containing 2 nM catalyst X_{cat} (e.g., X-6), 20 nM CP, and 20 nM Y; B_{cat} is the background from the same reaction mixture but no catalyst was added. To quantitatively characterize the efficacy of the allosteric regulator, an apparent dissociation constant K_d was defined as the equilibrium concentration of R when the amount of PR reaches to half of its maximum and estimated using a one-site binding hyperbola (eq 3):

$$\frac{[PR]}{[PR]_{max}} = \frac{[R]}{K_d + [R]} \quad (3)$$

RESULTS AND DISCUSSION

Enabling A-Toehold-Mediated Strand Displacement Using Mg^{2+}. We first set out to determine experimental conditions that enable A-toehold-mediated strand displacement reactions by using a strand displacement beacon. The displacement beacon was made by labeling C and P with a fluorophore and a quencher, respectively (Figure 1A). Strand displacement reactions can thus be monitored in real-time by measuring fluorescence signals generated by the beacon. As shown in Figure 1B, no obvious strand displacement was observed between CP and X in TE buffer (0 mM Mg^{2+}), suggesting that the overall reaction was likely to be limited by reaction 1 which is known to be thermodynamically disfavored. We then found that it is possible to overcome this thermodynamic barrier and activate A-toehold-mediated strand displacement by stabilizing CPR triplex using divalent metal cation Mg^{2+}. Moreover, the effect of Mg^{2+} is concentration dependent, and the rate of strand displacement increases when varying $[Mg^{2+}]$ from 5 mM to 100 mM (Figure 1B). The kinetic enhancement saturated when $[Mg^{2+}]$ reached 100 mM. TE buffer containing 100 mM Mg^{2+} was then used for all other experiments to ensure that Mg^{2+} was not a rate-limiting reagent. But it is also possible to tune the kinetics of A-toehold-mediated strand displacement by simply adjusting the concentration of Mg^{2+}. A-toehold-mediated strand displacement enabled by 100 mM Mg^{2+} was further confirmed using native polyacrylamide gel electrophoresis (Figure S1).

Tuning the Kinetics of Strand Displacement Reactions Using A-Toehold. Although A-toehold (domain 1* in Scheme 1B) is much less efficient than an equal amount of its toehold counterpart (domain 1* in Scheme 1A) (Figure S2), it is possible to promote the kinetic and analytical performance of A-toehold-mediated strand displacement to be close to its toehold-mediated strand displacement counterpart by raising the concentration of allosteric regulator R from 10 nM (Figure S2) to 250 nM (Figure S3). When [R] is in large excess, A-toehold-mediated strand displacement is effectively a second-order reaction (Figure 2). By fitting the kinetic data into the second-order rate equation (eq 1), we determined the effective rate constant k_{eff} to be 2.6×10^5 M^{-1} s^{-1} (Figure 2B), which is in the same order of magnitude with that of a 6-nt long regular toehold ($k_{\{0,6\}} = 5 \times 10^5$ M^{-1} s^{-1} as predicted by Zhang et al.[14a]).

Similar to toehold-mediated DNA strand displacement, the rate constant k_{eff} was also found to increase exponentially when varying the A-toehold length (domain 1*) m from 4 nt to 7 nt

DOI: 10.1021/jacs.6b08794
J. Am. Chem. Soc. 2016, 138, 14076−14082

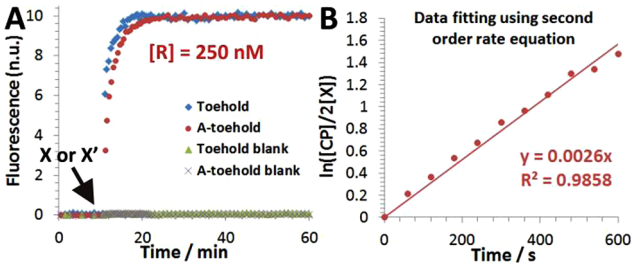

Figure 2. Kinetic profile of A-toehold-mediated DNA strand displacement. (A) Comparing A-toehold-mediated DNA strand displacement (red trace) with its toehold-mediated strand displacement counterpart (blue trace). CP was used for both reactions. X′ was used as an input for toehold-mediated strand displacement, whereas X and R were used to trigger A-toehold-mediated strand displacement. [X] = [X′] = 10 nM; [CP] = 20 nM; [R1] = 250 nM. (B) Determination of the effective rate constant k_{eff} by plotting $\ln([CP][X]_0/[X][CP]_0)$ (equal to $\ln([CP]/2[X])$) as a function of time and fitting the data using least-squares linear regression.

(Figure 3A). This feature allows the coarse-tuning of the reaction rates of A-toehold-mediated strand displacement. The

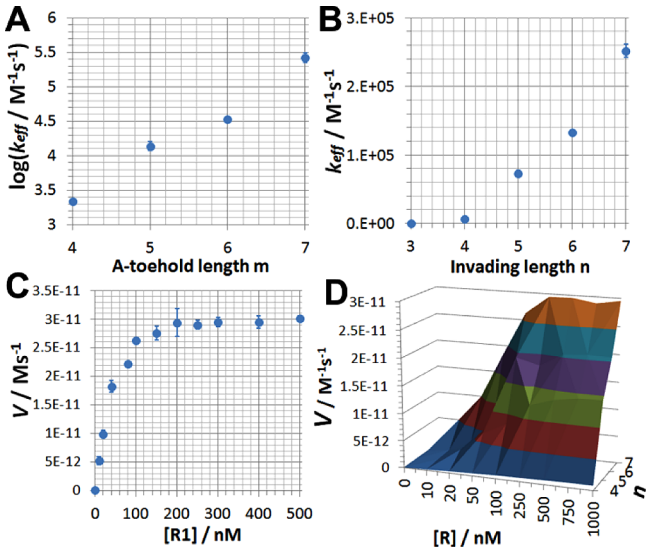

Figure 3. Tuning the kinetics of the DNA strand displacement using the allosteric DNA toehold. (A) Coarse-tuning of the effective rate constant k_{eff} by adjusting A-toehold length m. n = 7; [R] = 250 nM. (B) Fine-tuning of k_{eff} by adjusting the length of the invading motif n. m = 7; [R] = 250 nM. (C) Fine-tuning of displacement rate V using [R]. n = 7; m = 7. (D) Continuous tuning the displacement rate V by combining the two orthogonal factors: n and $[R]$ (m = 7). For all experiments, [X] = 10 nM, [CP] = 20 nM. Error bars represent one standard deviation from triplicate analyses.

design that A-toehold is split from the BM domain also allows additional fine-tuning of strand displacement kinetics through two more orthogonal factors: the length of the invading motif (domain 2*) n and the concentration of the regulator R ([R]).

To examine the feasibility of using A-toehold to fine-tune the rates of strand displacement, we first fixed the A-toehold length m (domain 1*) to be 7 nt and varied invading length (domain 2*) n from 3 to 10 nt. As shown in Figure 3B, a linear increase in k_{eff} was observed when varying n from 4 nt to 7 nt. Further increasing n from 7 to 10 nt was found to reduce the displacement rates (Figure S4). The decreases in displacement rates can be attributed to the unintended hybridization between X and R (X + R ↔ XR) through domain 2 and 2*, which sequesters X from reacting with CPR (reaction 2).

We then fixed both A-toehold and invading motif to be 7 nt long and tuned the kinetics of strand displacement using [R]. As shown in Figure 3C, the initial displacement rate V between X and CP increases linearly when varying [R] from 10 nM to 100 nM and saturated when [R] is greater than 200 nM. We then estimated the concentrations of stable CPR using NUPACK by setting the parameters to be the same as our experimental conditions. We found that even when displacement rate was saturated, the conversion from CP to CPR was less than 20% under our experimental conditions ([R] < 250 nM). A nearly complete conversion (90%) requires R to be at least 10 μM and a 50% conversion can be reached when [R] = 1 μM.

It was also found that when [R] was above 40 nM, adjustment of the kinetics of A-toehold reactions would not significantly alter the equilibrium concentration of the product XC (Figure S5). Moreover, manipulation of [R] is continuous, thus allowing the continuous fine-tuning of the displacement rates. Collectively, the rate of any A-toehold-mediated strand displacement can be regulated independently from the BM domain by a set of three parameters, m, n, and [R] (Figure 3D). This feature can be very useful for simplifying the design and dynamic regulation of various DNA devices and systems.

Dynamic Regulation of Strand Displacement Using A-Toehold. To demonstrate the dynamic regulation of DNA strand displacement using A-toehold, we designed an inhibitor I that is fully complementary to the regulator R, so that the effective concentration of R decreases in the presence of I (Figure 4A). The progress of strand displacement between X

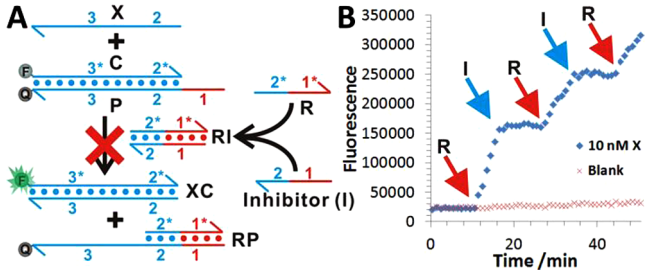

Figure 4. Dynamic regulation of DNA strand displacement using A-toehold strategy. (A) Schematic illustration of the inhibition of A-toehold-mediated DNA strand displacement by quenching the active A-toehold regulator R using an inhibitor strand I. (B) Real-time monitoring of fluorescence signals in response to the addition of R or I. [X] = 10 nM, [CP] = 20 nM, $[R]_{eff}$ = 20 nM, $[I]_{eff}$ = 20 nM ($[R]_{eff}$ and $[I]_{eff}$ are effective concentrations of R and I in the final solution).

and CP can then be modulated by the addition of R or I. As shown in Figure 4B, strand displacement between X and CP was completely turned off when I was in excess and restored when R was in excess. Moreover, the regulation on strand displacement kinetics through A-toehold is reversible and in real-time, evidenced by the sharp fluorescence changes upon the alternate addition of R or I. Compared to the dynamic allosteric control strategy described by Zhang and Winfree,[12] where dynamic regulation was achieved by controlled activation of an input strand, A-toehold strategy allows the direct regulation of gate molecules. It is more flexible to control a

DOI: 10.1021/jacs.6b08794
J. Am. Chem. Soc. 2016, 138, 14076−14082

gate component rather than an input, as inputs are typically the target molecules with predefined sequences.

Selective Activation of Multiple Strand Displacement Reactions Using A-Toeholds. Another advantage of splitting toehold and BM from a single input strand is the possibility to achieve the selective activation of a specific strand displacement reaction from a mixture of multiple substrates using the same BM sequence but with a specific A-toehold. A similar concept, such as combinatorial displacement, has previously been demonstrated by Genot et al. to achieve matrix multiplication and weighted sums.[13] The selective activation of combinatorial displacement was built on the associative toehold design and thus requiring a DNA hybridization event to attach a specific toehold to a BM domain.[13] Our A-toehold design has the potential to simplify the selective activation process by eliminating the need for additional hybridization domains to attach toehold and BM motifs. To demonstrate the potential uses of A-toehold in such applications, we designed two displacement beacons by labeling C with two distinct fluorescent dyes, 6-FAM (C1) and TAMRA (C2), respectively (Figure 5A). The complementary protecting sequence P1 and P2 are of two different toehold domains (domain 1 for P1 and domain 5 for P2). R1 is designed to contain the specific A-toehold for C1P1 (domain 1*), whereas R2 is designed for C2P2 (containing domain 5*). Equal concentrations of C1P1 and C2P2 (20 nM each) were then mixed together with 10 nM X. By measuring the two fluorescent channels in parallel (Figure 5B–D), we observed that the displacement reactions between X and CP were highly specific. The selectivity was strictly controlled by the A-toehold sequence on R. Moreover, the selective activation can also be achieved in a quantitative manner by simply adjusting the ratio between specific A-toehold regulators (Figure 5C and Figure S6).

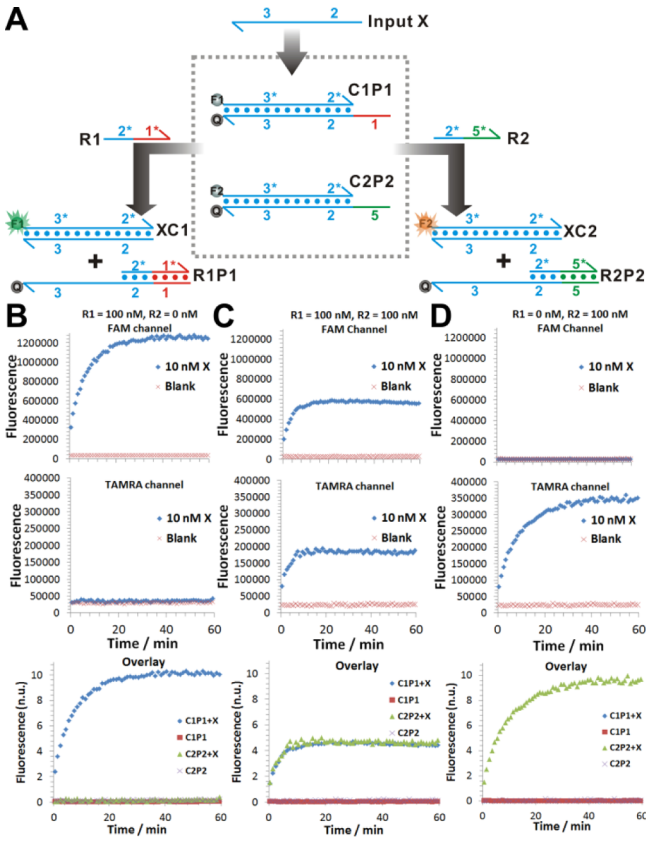

Figure 5. (A) Schematic illustration of the selective activation of multiple displacement reactions using A-toehold regulators. (B–D) Real-time monitoring of fluorescence signals generated by strand displacement reactions activated by R1 (FAM channel) and/or R2 (TAMRA channel). The overlay plots were obtained by normalizing raw fluorescence signals against fluorescence of 100 nM R1 or R2 and 0 nM R1 or R2 as P.C. and N.C. at t = 60 min. [X] = 10 nM; [C1P1] = [C2P2] = 20 nM.

Activation of Toehold-Exchange Reactions using A-Toehold. Having demonstrated A-toehold strategy on dynamic and selective regulation of DNA strand displacement reactions, we aim to further expand this strategy to DNA devices with higher structural complexity. Because toehold-exchange is one of the most widely used mechanisms to construct complexed DNA devices or circuits,[14] we first examined the adaptability of our A-toehold design to toehold-exchange reactions. As shown in Figure 6, A-toehold was able to trigger toehold-exchange

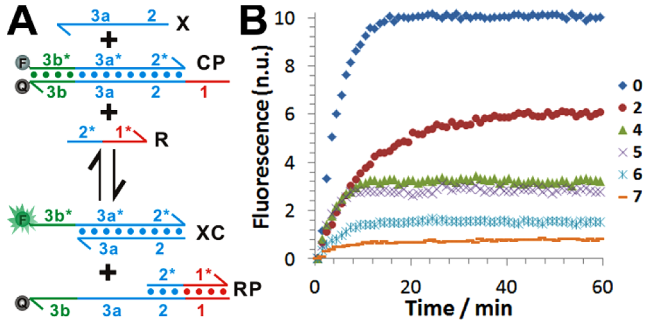

Figure 6. (A) Schematic illustration of A-toehold-mediated toehold-exchange reactions. (B) Fluorescence signals generated by toehold-exchange reactions that are of varying reverse toehold length r from 0 to 7 nt. [X-r] = 10 nM; [CP] = 20 nM; [R1] = 250 nM.

reactions with the reverse toehold (domain 3b/3b*) r ranging from 0 to 7 nt. A clear shift was also observed on the reaction equilibrium toward the reactants when increasing r from 0 nt to 7 nt (Figure 6B), suggesting that A-toehold-mediated toehold-exchange reactions are reversible and thus are adaptable to the construction of catalytic DNA circuits. Encouraged by this result, we developed an A-toehold-mediated noncovalent DNA catalysis network that resembled an allosteric enzyme.

A-Toehold-Mediated Noncovalent DNA Catalysis. Figure 7A shows the mechanism of A-toehold-mediated DNA catalysis. CP reacts with R, forming reaction intermediate CPR triplex. The catalyst X_{cat} (e.g., X-6) then hybridizes and initiates a branch migration with CPR, leading to the production of $X_{cat}C$. Once $X_{cat}C$ forms, it then reacts with Y through a toehold-exchange mechanism, yielding the product CY. Meanwhile, X_{cat} is released back into the solution and can then be used to catalyze the next cycle of toehold-exchange with CPR. Because R activates the overall reaction but does not involve in the catalytic center, mimicking the role of an allosteric effector, A-toehold-mediated DNA catalysis hence resembles an allosteric enzyme.

To construct A-toehold-mediated DNA catalysis, we first systematically characterized a set of design parameters, including allosteric regulator R (Figure S7), substrate Y (Figure S8), and catalyst X_{cat} (Figure S9). The optimal design was achieved when R-8-7 and X-6 were used as the regulator and the catalyst, and Y had an optimal concentration of 20 nM (details in the Supporting Information). The optimal result is

DOI: 10.1021/jacs.6b08794
J. Am. Chem. Soc. 2016, 138, 14076–14082

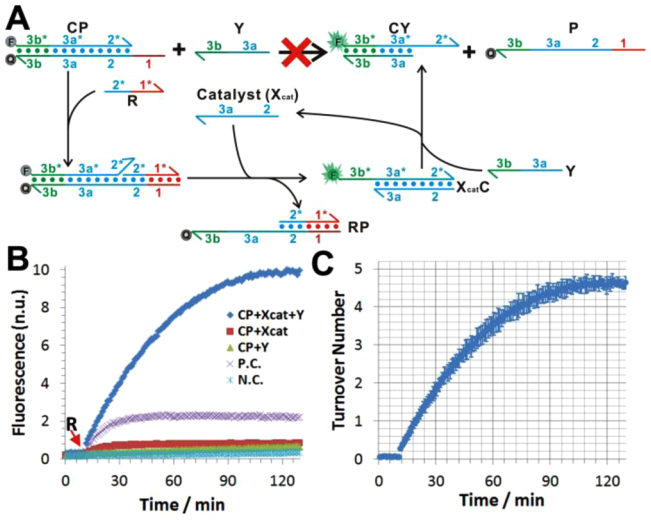

Figure 7. (A) Schematic illustration of the activation of noncovalent DNA catalysis using the allosteric DNA regulator. (B) Real-time monitoring of DNA catalysis activation and progression. For DNA catalysis: [X-6] = 2 nM; [Y] = 20 nM; [CP] = 20 nM; [R-8-7] = 150 nM. For controls: [X] = 2 nM; [CP] = 20 nM; [R1] = 250 nM. (C) TON as a function of reaction time. TON at each time point was determined using eq 2. Error bars represent one standard deviation from triplicate analyses.

shown in Figure 7B. DNA catalysis was activated by 150 nM R-8-7 and mediated by 2 nM catalyst X-6. A TON of ~4.5 was achieved over a period of 120 min (Figure 7C). The determined TON can be overestimated by up to 1, as intermediate $X_{cat}C$ also contributed to the fluorescence signal.

R-8-7 was also found to regulate both kinetics and thermodynamics of the DNA catalysis in a concentration-dependent manner (Figure S10A). We reason that because the role of R-8-7 resembles an allosteric effector, it is possible to quantitatively characterize R-8-7 using a dissociation constant that is commonly used to describe the efficacy of allosteric effectors.[15] We then defined an apparent dissociation constant K_d, which represents the equilibrium concentration of R-8-7 when RP reaches half of its maximum amount (when R-8-7 is saturated). The binding curve is shown in Figure S10B. By using a one-site binding hyperbola fitting, we determined the apparent K_d of R-8-7 to be (14.3 ± 1.7) nM.

CONCLUSION

Since the introduction of DNA toehold in 2000, the boom of dynamic DNA nanotechnology has been driven largely by the development of new toehold designs and new strand displacement schemes. For example, the development of the toehold-exchange principle enables the development of highly complexed DNA circuit networks and ultraspecific DNA sensors.[14] The cooperative hybridization achieved by dual toehold-exchange reactions demonstrates great potential for material assembly.[14b] The development of associative toehold greatly expands the rule set of DNA circuitry.[8] The "hidden" toehold,[16] binding-induced toehold,[10] photoactivated toehold,[17] pH-regulated toehold,[18] and metallic toehold[19] expand DNA devices from the realm of nucleic acids to non-nucleic-acid inputs.

Here the allosteric DNA toehold (A-toehold) strategy is a new addition to the current toolbox of DNA strand displacement techniques. It has the potential to simplify DNA sequence designs to achieve dynamic and selective control of DNA strand displacement. It is also adaptable to other toehold activation mechanisms and thus could be used in combination with other strand displacement strategies to build complexed DNA devices or circuits. For example, we have demonstrated an allosteric DNA catalysis system which was achieved by combining A-toehold with toehold-exchange mechanisms.

It is also possible to integrate the A-toehold principle into more complex DNA networks than demonstrated in this work. For example, A-toehold may be used as a threshold element in seesaw DNA gates to facilitate the construction of strand displacement cascades.[2f,g] To achieve this goal, it is critical to improve the composability of A-toehold through flexible output designs. For example, RP can be modified to serve as an output strand for subsequent strand displacement events by extending the 3* domain of P with new domains and sequestering the toehold motif (part of the 3* domain) into CP. XC can also serve as an associative output by extending both X and C with additional domains (e.g., a toehold domain on X and a BM domain on C), so that subsequent strand displacement could not occur until XC forms. It is also necessary to establish a more sophisticated kinetic model that includes each individual reaction and each rate constant and simulate the model with mass-action kinetics. Better understanding of A-toehold reactions will help guide their future uses in DNA nanotechnology and beyond.

ASSOCIATED CONTENT

Supporting Information

The Supporting Information is available free of charge on the ACS Publications website at DOI: 10.1021/jacs.6b08794.

Table S1 and Figures S1–S10 (PDF)

AUTHOR INFORMATION

Corresponding Author

*fli@brocku.ca

Notes

The authors declare no competing financial interest.

ACKNOWLEDGMENTS

We thank Dr. Milan Stojanovic and anonymous reviewers for their insightful suggestions and comments. We thank the National Sciences and Engineering Research Council of Canada and the Brock University Start-Up Fund for financial support.

REFERENCES

(1) (a) Jones, M. R.; Seeman, N. C.; Mirkin, C. A. *Science* **2015**, *347*, 1260901. (b) Zhang, D. Y.; Seelig, G. *Nat. Chem.* **2011**, *3*, 103–113. (c) Aldaye, F. A.; Palmer, A. L.; Sleiman, H. F. *Science* **2008**, *321*, 1795–1799.

(2) (a) Seelig, G.; Soloveichik, D.; Zhang, D. Y.; Winfree, E. *Science* **2006**, *314*, 1585–1588. (b) Soloveichik, D.; Seelig, G.; Winfree, E. *Proc. Natl. Acad. Sci. U. S. A.* **2010**, *107*, 5393–5398. (c) Chen, Y.-J.; Dalchau, N.; Srinivas, N.; Phillips, A.; Cardelli, L.; Soloveichik, D.; Seelig, G. *Nat. Nanotechnol.* **2013**, *8*, 755–762. (d) Yin, P.; Choi, H. M. T.; Calvert, C. R.; Pierce, N. A. *Nature* **2008**, *451*, 318–322. (e) Zhang, D. Y.; Turberfield, A. J.; Yurke, B.; Winfree, E. *Science* **2007**, *318*, 1121–1125. (f) Qian, L.; Winfree, E. *Science* **2011**, *332*, 1196–1201. (g) Qian, L.; Winfree, E.; Bruck, J. *Nature* **2011**, *475*, 368–372. (h) Jung, C.; Ellington, A. D. *Acc. Chem. Res.* **2014**, *47*, 1825–1835. (i) Stojanovic, M. N.; Stefanovic, D.; Rudchenko, S. *Acc. Chem. Res.* **2014**, *47*, 1845–1852.

DOI: 10.1021/jacs.6b08794
J. Am. Chem. Soc. 2016, 138, 14076–14082

(3) (a) Bath, J.; Turberfield, A. J. *Nat. Nanotechnol.* **2007**, *2*, 275−284. (b) He, Y.; Liu, D. R. *Nat. Nanotechnol.* **2010**, *5*, 778−782. (c) Jung, C.; Allen, P. B.; Ellington, A. D. *Nat. Nanotechnol.* **2016**, *11*, 157−163. (d) Han, X.; Zhou, Z.; Yang, F.; Deng, Z. *J. Am. Chem. Soc.* **2008**, *130*, 14414−14415. (e) Lund, K.; Manzo, A. J.; Dabby, N.; et al. *Nature* **2010**, *465*, 206−210. (f) Liu, M.; Fu, J.; Hejesen, C.; Yang, Y.; Woodbury, N. W.; Gothelf, K.; Liu, Y.; Yan, H. *Nat. Commun.* **2013**, *4*, 2127.

(4) (a) Zhang, H.; Li, F.; Dever, B.; Li, X.-F.; Le, X. C. *Chem. Rev.* **2013**, *113*, 2812−2841. (b) You, M.; Zhu, G.; Chen, T.; Donovan, M. J.; Tan, W. *J. Am. Chem. Soc.* **2015**, *137*, 667−674. (c) Yang, X.; Tang, Y.; Mason, S. D.; Chen, J.; Li, F. *ACS Nano* **2016**, *10*, 2324−2330. (d) Tang, Y.; Lin, Y.; Yang, X.; Wang, Z.; Le, X. C.; Li, F. *Anal. Chem.* **2015**, *87*, 8063−8066. (e) Tang, Y.; Wang, Z.; Yang, X.; Chen, J.; Liu, L.; Zhao, W.; Le, X. C.; Li, F. *Chem. Sci.* **2015**, *6*, 5729−5733. (f) Li, Q.; Luan, G.; Guo, Q.; Liang, J. *Nucleic Acid Res.* **2002**, *30*, e5.

(5) (a) Liu, Z.; Lu, C.-H.; Willner, I. *Acc. Chem. Res.* **2014**, *47*, 1673−1680. (b) Goodman, R. P.; Heilemann, M.; Doose, S.; Erben, C. M.; Kapanidis, A. N.; Turberfield, A. J. *Nat. Nanotechnol.* **2008**, *3*, 93−96.

(6) Reynaldo, L. P.; Vologodskii, A. V.; Neri, B. P.; Lyamichev, V. I. *J. Mol. Biol.* **2000**, *297*, 511−520.

(7) Yurke, B.; Turberfield, A. J.; Mills, A. P., Jr; Simmel, F. C.; Neumann, J. L. *Nature* **2000**, *406*, 605−608.

(8) Chen, X. *J. Am. Chem. Soc.* **2012**, *134*, 263−271.

(9) (a) Li, B.; Jiang, Y.; Chen, X.; Ellington, A. D. J. *J. Am. Chem. Soc.* **2012**, *134*, 13918−13921. (b) Guo, Y.; Wu, J.; Ju, H. *Chem. Sci.* **2015**, *6*, 4318−4323.

(10) (a) Li, F.; Zhang, H.; Wang, Z.; Li, X.-F.; Li, X.; Le, X. C. *J. Am. Chem. Soc.* **2013**, *135*, 2443−2446. (b) Li, F.; Zhang, H.; Lai, C.; Li, X.-F.; Le, X. C. *Angew. Chem., Int. Ed.* **2012**, *51*, 9317−9320. (c) Li, F.; Lin, Y.; Le, X. C. *Anal. Chem.* **2013**, *85*, 10835−10841.

(11) Genot, A. J.; Zhang, D. Y.; Bath, J.; Turberfield, A. J. *J. Am. Chem. Soc.* **2011**, *133*, 2177−2182.

(12) Zhang, D. Y.; Winfree, E. *J. Am. Chem. Soc.* **2008**, *130*, 13921−13926.

(13) Genot, A. J.; Bath, J.; Turberfield, A. J. *Angew. Chem., Int. Ed.* **2013**, *52*, 1189−1192.

(14) (a) Zhang, D. Y.; Winfree, E. *J. Am. Chem. Soc.* **2009**, *131*, 17303−17314. (b) Zhang, D. Y. *J. Am. Chem. Soc.* **2011**, *133*, 1077−1086. (c) Chen, S. X.; Zhang, D. Y.; Seelig, G. *Nat. Chem.* **2013**, *5*, 782−789. (d) Wang, J. S.; Zhang, D. Y. *Nat. Chem.* **2015**, *7*, 545−553. (e) Wu, L. R.; Wang, J. S.; Fang, J. Z.; R Evans, E.; Pinto, A.; Pekker, I.; Boykin, R.; Ngouenet, C.; Webster, P. J.; Beechem, J.; Zhang, D. Y. *Nat. Methods* **2015**, *12*, 1191−1196. (f) Wang, C.; Bae, J. H.; Zhang, D. Y. *Nat. Commun.* **2016**, *7*, 10319.

(15) (a) Goodey, N. M.; Benkovic, S. J. *Nat. Chem. Biol.* **2008**, *4*, 474−482. (b) Wang, D. Y.; Lai, B. H. Y.; Feldman, A. R.; Sen, D. *Nucleic Acid Res.* **2002**, *30*, 1735−1742.

(16) Xing, Y.; Yang, Z.; Liu, D. *Angew. Chem., Int. Ed.* **2011**, *50*, 11934−11936.

(17) Huang, F.; You, M.; Han, D.; Xiong, X.; Liang, H.; Tan, W. *J. Am. Chem. Soc.* **2013**, *135*, 7967−7973.

(18) (a) Dong, Y.; Yang, Z.; Liu, D. *Acc. Chem. Res.* **2014**, *47*, 1853−1860. (b) Porchetta, A.; Idili, A.; Ballee-Belisle, A.; Ricci, F. *Nano Lett.* **2015**, *15*, 4467−4471. (c) Idili, A.; Porchetta, A.; Amodio, A.; Ballee-Belisle, A.; Ricci, F. *Nano Lett.* **2015**, *15*, 5539−5544.

(19) (a) Porchetta, A.; Ballee-Belisle, A.; Plaxco, K. W.; Ricci, F. *J. Am. Chem. Soc.* **2013**, *135*, 13238−13241. (b) Tang, W.; Wang, H.; Wang, D.; Zhao, Y.; Li, N.; Liu, F. J. *J. Am. Chem. Soc.* **2013**, *135*, 13628−13631.

DOI: 10.1021/jacs.6b08794
J. Am. Chem. Soc. 2016, 138, 14076−14082